Chapter 1

Point-to-Point versus Mobile Wireless Communication Channels

1.1 BANDPASS MODEL FOR POINT-TO-POINT COMMUNICATIONS

In this section we provide a brief review of the standard bandpass link model for point-to-point communications. This model has driven the design of the physical layer of most wireline communication networks.

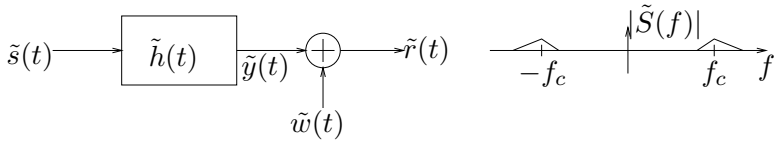

Figure 1.1: Real bandpass model for point-to-point communications.

Most point-to-point communication links (e.g., the telephone line channel, fixed microwave channels, etc.) are well-modeled using a bandpass additive noise system model of the form shown in Figure 1.1. All the signals in this model are written with "tildas" which will be dropped in the complex baseband representation of the following section. A more detailed description of the link model is as follows:

- The message bearing signal $\tilde{s}(t)$ is generally a carrier-modulated real-valued signal, with carrier frequency f_c. Hence its Fourier spectrum $\tilde{S}(f)$ is concentrated[1] in the vicinity of f_c. The bandwidth W of the signal is such that $W \ll f_c$.
- Distortions introduced by the channel are usually well-approximated by a linear *time-invariant* system with impulse response $\tilde{h}(t)$, and frequency response $\tilde{H}(f)$ that is concentrated around f_c. The channel response $\tilde{h}(t)$ may or may not be known at the receiver. In the simplest case, $\tilde{h}(t)$ corresponds to an ideal bandpass filter with bandwidth corresponding to that of the signal $\tilde{s}(t)$.

[1]There is of course the special case where the signal is not carrier modulated, and $\tilde{S}(f)$ is then concentrated around $f = 0$. We will not be concerned with this special case in much of this book since all practical wireless signals are carrier modulated. One exception is ultra-wideband communications that will be discussed in Chapter **??**.

Passband to Baseband	Baseband to Passband
$S(f) = \tilde{S}_+(f+f_c) = \sqrt{2}u(f+f_c)\tilde{S}(f+f_c)$	$\tilde{S}(f) = \frac{S(f-f_c)+S^\star(-f-f_c)}{\sqrt{2}}$
$s(t) = \tilde{s}_+(t)e^{-j2\pi f_c t} = \frac{1}{\sqrt{2}}[\tilde{s}(t) + j\hat{\tilde{s}}(t)]e^{-j2\pi f_c t}$	$\tilde{s}(t) = \mathsf{Re}[\sqrt{2}s(t)e^{j2\pi f_c t}]$
$h(t) = \frac{1}{\sqrt{2}}\tilde{h}_+(t)e^{-j2\pi f_c t}$	$\tilde{h}(t) = 2\mathsf{Re}[h(t)e^{j2\pi f_c t}]$
$w(t) = \tilde{w}_+(t)e^{-j2\pi f_c t} = \frac{1}{\sqrt{2}}[\tilde{w}(t) + j\hat{\tilde{w}}(t)]e^{-j2\pi f_c t}$	$\tilde{w}(t) = \mathsf{Re}[\sqrt{2}w(t)e^{j2\pi f_c t}]$

Table 1.1: Passband-Baseband Relationships

- The additive noise signal $\tilde{w}(t)$ is a *Wide Sense Stationary* (WSS) bandpass random process. It is usually idealized by *White Gaussian Noise* (WGN) for the purposes of analysis.
- The received signal $\tilde{r}(t)$ is a real-valued bandpass process as well.

1.2 COMPLEX BASEBAND MODEL FOR POINT-TO-POINT COMMUNICATIONS

As shown in Appendix A, we can convert each component in the system model of Figure 1.1 into its corresponding complex baseband equivalent. The relationships between the passband and baseband quantities are presented in Table 1.2. In the table, the quantities with "tildas" denote bandpass versions, and the corresponding ones without "tildas" denote baseband versions. The representations for $y(t)$ and $r(t)$ are analogous to those for $s(t)$ (and $S(f)$) and have not been included in the table. Based on these representations, we

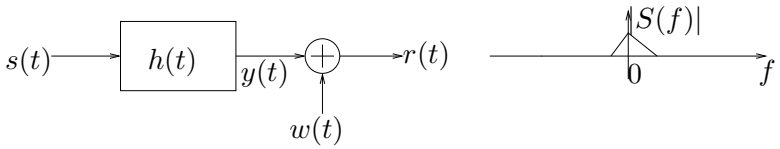

Figure 1.2: Complex baseband model for point-to-point communications.

then have the complex baseband system shown in Figure 1.2 which is equivalent to the bandpass system of Figure 1.1. Note that the baseband channel h satifies the standard linear time-invariant model:

$$y(t) = h * s(t) = \int h(\tau)\ s(t-\tau)\ d\tau\ . \tag{1.1}$$

1.2.1 COMPLEX BASEBAND NOISE

The complex process $w(t)$ inherits several interesting properties from corresponding bandpass noise process $\tilde{w}(t)$. We now explore these properties.

First, if $\tilde{w}(t)$ is zero mean, then $w(t)$ is obviously zero mean as well. Furthermore, if we assume that $\tilde{w}(t)$ is a wide sense stationary (WSS) process (see Section **??**), then this assumption induces a remarkable structure in the process $w(t)$. To explain this structure, we rewrite $w(t)$ as

$$w(t) = w_I(t) + jw_Q(t) \,, \tag{1.2}$$

where $w_I(t)$ and $w_Q(t)$ are the real in-phase and quadrature components, respectively. Referring to (A.17), we see that since the Hilbert transform is a linear operation, the processes $\tilde{w}(t)$ and $\hat{\tilde{w}}(t)$ are jointly WSS [WH85]. This implies that $w_I(t)$ and $w_Q(t)$ are jointly WSS as well. Furthermore, we it is easy to show that the auto- and cross-correlation functions satisfy[2]

$$R_{w_I}(\xi) = R_{w_Q}(\xi) \,, \quad \text{and } \; R_{w_I w_Q}(\xi) = -R_{w_Q w_I}(\xi) \,. \tag{1.3}$$

A complex process with in-phase and quadrature components that satisfy the above property is said to be a *proper complex* process. We study such processes in greater detail later in Appendix B. It is interesting to note that proper complex processes arise in a very different context in the study of small scale fading in Chapter **??**.

The autocorrelation function (ACF) of a complex process $Y(t)$ is defined as:

$$R_Y(t+\xi, t) = \mathsf{E}[Y(t+\xi)Y^\star(t)] \,. \tag{1.4}$$

If $\mathsf{E}[Y(t)]$ and $R_Y(t+\xi, t)$ are independent of t, then $Y(t)$ is said to be wide sense stationary (WSS), and we write $R_Y(t+\xi, t) = R_Y(\xi)$. For WSS $Y(t)$, the power spectral density (PSD) is defined as the Fourier transform of $R_Y(\xi)$.

From (1.3), it is easy to show that the ACF of $w(t)$ is given by

$$R_w(t+\xi, t) = 2R_{w_I}(\xi) + j\; 2R_{w_Q w_I}(\xi) = R_w(\xi) \,. \tag{1.5}$$

Hence $w(t)$ is a zero-mean complex WSS process. Furthermore, starting from (A.17), we can show that

$$R_{\tilde{w}}(\xi) = \mathsf{Re}[R_w(\xi)\, e^{j2\pi f_c \xi}] \,. \tag{1.6}$$

The power spectral densities of $\tilde{w}(t)$ and $w(t)$ are hence related as:

$$S_{\tilde{w}}(f) = \frac{1}{2}\left[S_w(f - f_c) + S_w(-f - f_c)\right] \,. \tag{1.7}$$

If $\tilde{w}(t)$ is a stationary *Gaussian* process, then the analysis given above shows that $w(t)$ has components $w_I(t)$ and $w_Q(t)$ that are jointly Gaussian and stationary, and satisfy (1.3). Such a process $w(t)$ said to be a stationary *proper complex Gaussian* (PCG) process. (See Appendix B.)

If $\{\tilde{w}(t)\}$ is idealized by a white Gaussian noise (WGN) process with spectral hieght $N_0/2$ in Figure 1.1, then the corresponding idealization for $w(t)$ can be shown to be a process with ACF

$$R_w(\xi) = N_0 \delta(\xi) \tag{1.8}$$

Since $R_w(\xi)$ is real, from (1.5) we see that $R_{w_I w_Q}(\xi)$ must be 0 for all ξ, i.e., in-phase and quadrature process are uncorrelated. Furthermore these processes have ACF's that are given by

$$R_{w_I}(\xi) = R_{w_Q}(\xi) = \frac{1}{2}\, R_w(\xi) = \frac{N_0}{2}\delta(\xi) \,. \tag{1.9}$$

[2]For jointly WSS random processes $X(t)$ and $Y(t)$, we define $R_X(\xi) = \mathsf{E}[X(t+\xi)X(t)]$, and $R_{XY}(\xi) = \mathsf{E}[X(t+\xi)Y(t)]$

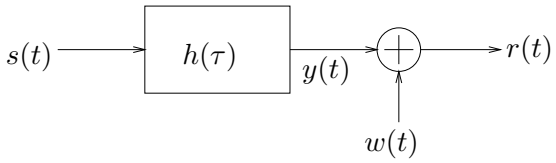

Figure 1.3: Complex baseband point-to-point link.

and PSD's that are given by

$$S_{w_I}(f) = S_{w_Q}(f) = \frac{1}{2} S_w(f) = \frac{N_0}{2} \text{ for all } f \,. \tag{1.10}$$

1.3 FROM POINT-TO-POINT LINK MODEL TO MOBILE WIRELESS LINK MODEL

In the previous section, we developed the baseband model for point-to-point communications shown in Figure 1.3. The goal of this book is to modify this model to incorporate the features of a mobile wireless communications link. The following are points worth noting in making the transition to the mobile communication link model.

- The additive noise term $w(t)$ is always present whether the channel is point-to-point or mobile, and usually $w(t)$ is well-modelled as a proper complex white Gaussian process. The additive noise term may include interference from other user sharing the spectrum and in this case the Gaussian model may not be accurate.

- For point-to-point communications the channel response is generally well modelled by a linear time-invariant (LTI) system ($h(\tau)$ may or may not be known at the receiver). For mobile communications, the channel response is time-varying, and we will see that it is well-modelled as a linear time-varying (LTV) system.

- The variations in the channel may arise from both the movement of the terminals as well as of the reflectors in the environment.

Consider the situation where the receiver is at location (x, y) or (d, ϑ) in a coordinate system with the transmitter at the origin as shown in Figure 1.4. The transmitted signal, may propagate to the receiver over several paths. If the direct (line-of-sight) path is not blocked, then this will be first to arrive at the receiver. In addition, there may be paths that are reflected off scatterers in the environment as shown in Figure 1.4. A 3-d description of location may be more appropriate in some situations (e.g., when mobiles could be located on various floors in a tall building), but for simplicity we will restrict our attention to the 2-d model[3]. Also, we restrict our attention now to the channel connecting one pair of transmit and receive antennas. The multiantenna channel model is considered in detail in Chapters **??** and **??**.

[3]The location model will be mainly relevant in the study of large scale channel variations in Chapter **??**, and the extension from a 2-d to a 3-d location model is straightforward but somewhat cumbersome.

If the receiver is fixed at location (d, ϑ), the channel that it sees is time-invariant. The response of this time-invariant channel is a function of the location, and is determined by all paths connecting the transmitter and the receiver. Thus we have the system shown in Figure 1.5, where $h_{d,\vartheta}(\tau)$ is the impulse response of a causal LTI system, which is a function of the multipath profile between the transmitter and receiver.

Referring to Figure 1.4, suppose there are a total of N paths connecting the transmitter and receiver, and suppose the n-th path has amplitude gain $\beta_n(d, \vartheta)$ and delay $\tau_n(d, \vartheta)$. The delay of $\tau_n(d, \vartheta)$ introduces a carrier phase shift, $\phi_n(d, \vartheta)$, which is given by

$$\phi_n(d, \vartheta) = -2\pi f_c \tau_n(d, \vartheta) + \text{constant} \tag{1.11}$$

where the constant depends on the reflectivity of the surface(s) that reflect the path. Thus we can write the output $y(t)$ in terms of the input $s(t)$ as

$$y(t) = \sum_{n=1}^{N} \beta_n(d, \vartheta)\ e^{j\phi_n(d,\vartheta)}\ s(t - \tau_n(d, \vartheta))\ , \tag{1.12}$$

which implies that the impulse response is

$$h_{d,\vartheta}(\tau) = \sum_{n=1}^{N} \beta_n(d, \vartheta)\ e^{j\phi_n(d,\vartheta)}\ \delta(t - \tau_n(d, \vartheta))\ . \tag{1.13}$$

That is

$$y(t) = \int\ h_{d,\vartheta}(\tau)\ s(t - \tau)\ d\tau\ . \tag{1.14}$$

Now supposing locations of the terminals change with time (or if the scatterers move). Then the linear system associated with the channel becomes time-varying. There are two scales of variation:

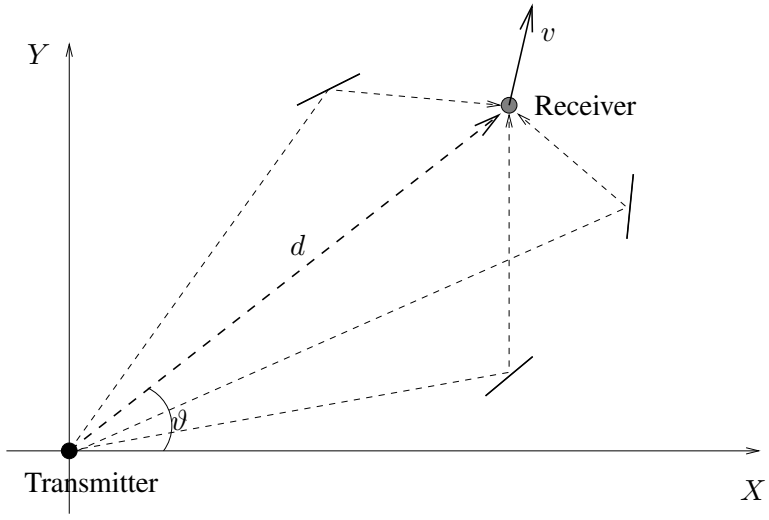

Figure 1.4: Multipath channel at location (d, ϑ) for one tranmit-receive antenna pair

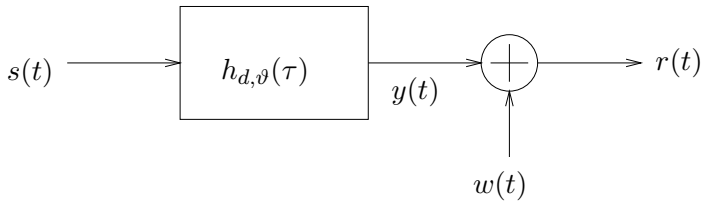

Figure 1.5: Causal LTI system representing multipath profile at location (d, ϑ)

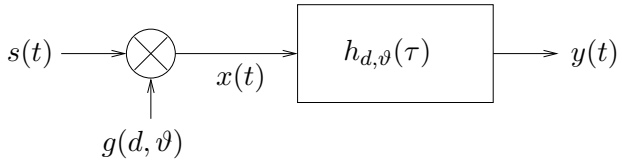

Figure 1.6: Small and large scale variation components of channel

The first is a small scale variation due to rapid changes in the phases ϕ_n for movements over distances of the order of the carrier wavelength λ_c which is given by

$$\lambda_c = \frac{c}{f_c}\,, \tag{1.15}$$

where c is the velocity of light. This is because movements in space of the order of a wavelength cause changes in τ_n of the order of $1/f_c$, which in turn cause changes in ϕ_n of the order of 2π. Note that for a 900 MHz carrier, which is typical for first and second generation cellular systems, $\lambda_c \approx 1/3$ m. For a 5 GHz carrier, λ_c is only 6 cm, which means that even small movements of a mobile terminal (say in the hands of the user) can cause large changes in the phase. We note that small scale variations may also occur when the terminals are stationary due to movements of the scatterers.

Modeling the phases ϕ_n as independent Uniform$[0, 2\pi]$ random variables (we elaborate on this assumption in Chapter **??**, Assumption **??**), we can see from (1.13) that the average power gain in the vicinity of (d, ϑ) is given by the sum of the squares of the path amplitudes. We denote this average power gain by $G(d, \vartheta)$, i.e.,

$$G(d, \vartheta) = \sum_{n=1}^{N} \beta_n^2(d, \vartheta)\,. \tag{1.16}$$

The second scale of variation is a large scale variation due to changes in $\{\beta_n(d, \vartheta)\}$ – both in the number of paths and their strengths. These changes happen on the scale of the distance between objects in the environment. Given that typical carrier wavelengths in cellular systems are of the order 10 cm or smaller, and that distances between objects in any realistic environment are of the order of 10 m or larger, we have a distinct separation between these scales of variation.

To study these two scales of variation separately, we redraw Figure 1.5 in terms of two components as shown in Figure 1.6. Here $h_{d,\vartheta}$ is normalized so that the average power gain introduced by $h_{d,\vartheta}$ is 1, i.e.

$$h_{d,\vartheta}(\tau) = \sum_{n=1}^{N} \beta_n(d, \vartheta)\, e^{j\phi_n(d,\vartheta)} \delta(\tau - \tau_n(d, \vartheta)) \tag{1.17}$$

where $\{\beta_n(d,\vartheta)\}$ is normalized so that $\sum_{n=1}^{N}\beta_n^2(d,\vartheta)=1$. The large scale variations in (average) amplitude gain are then lumped into the multiplicative term $g(d,\vartheta)$. The large scale variations in power gain are given in terms of $g(d,\vartheta)$ as

$$G(d,\vartheta)=g^2(d,\vartheta)\ . \tag{1.18}$$

Remark 1.1. *The channel between the terminals is symmetric in that it remains the same if we swap the receiver and transmitter. However, it is often the case (for example in cellular systems) that the two terminals transmit (and receive) with different carrier frequencies. The large scale variation component of the channel is insensitive to the carrier frequency, whereas the small scale variation component is strong function of the carrier frequency. Thus, if different carrier frequencies are different, the large scale variations can be assumed to be identical on both links, but the small scale variations will behave quite differently.*

Appendix A

Baseband-Passband Relationships

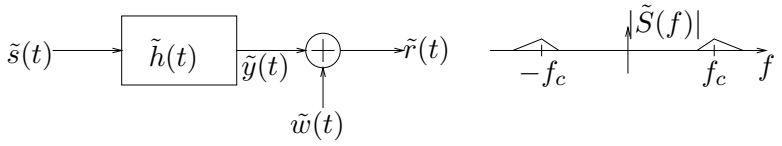

Figure A.1: Real bandpass model for point-to-point communications.

To convert the bandpass system model shown Figure A.1 into its equivalent complex baseband model, we take an approach similar to the one given in Chapter 4 of Proakis[Pro95] to represent each component.

We begin with the representation of the signal.

A.1 COMPLEX BASEBAND REPRESENTATION FOR SIGNAL

Since $\tilde{s}(t)$ is real, its Fourier spectrum $\tilde{S}(f)$ is symmetric about $f = 0$. Hence all of the information about $\tilde{s}(t)$ is contained in $\tilde{S}(f)$ for $f \geq 0$, which we define as

$$\tilde{S}_+(f) = \sqrt{2}\, \tilde{S}(f)u(f)\,. \tag{A.1}$$

where $u(\cdot)$ is the unit step function. The inverse Fourier transform of $\tilde{S}_+(f)$ is easily shown to be the complex signal

$$\tilde{s}_+(t) = \frac{1}{\sqrt{2}}[\tilde{s}(t) + j\hat{\tilde{s}}(t)]\,, \tag{A.2}$$

where $\hat{\tilde{s}}(t)$ is the Hilbert transform[1] of $\tilde{s}(t)$. The signal $\tilde{s}_+(t)$ is called the *pre-envelope* of $\tilde{s}(t)$. The factor of $\sqrt{2}$ in (A.1) ensures that $\tilde{s}_+(t)$ has the same energy as $\tilde{s}(t)$.

If we shift the spectrum of $\tilde{S}_+(f)$ down to the origin, we get the baseband spectrum

$$S(f) = \tilde{S}_+(f + f_c)\,, \tag{A.3}$$

[1]The Hilbert transform of a signal $x(t)$ is denoted by $\hat{x}(t)$, and is defined via its Fourier transform as $\hat{X}(f) = j\text{sgn}(f)X(f)$.

whose inverse Fourier transform is the baseband signal $s(t)$,

$$s(t) = \tilde{s}_+(t)\, e^{-j2\pi f_c t} \,. \tag{A.4}$$

Note that since $S(f)$ is not necessarily symmetric around the origin, $s(t)$ is in general complex-valued. The signal $s(t)$ is called the *complex envelope* or the *complex baseband representation* of the real signal $\tilde{s}(t)$. From (A.2) and (A.4), we get

$$\begin{aligned} \tilde{s}(t) &= \mathsf{Re}[\sqrt{2}\,\tilde{s}_+(t)] \\ &= \mathsf{Re}[\sqrt{2}\,s(t)e^{j2\pi f_c t}] \,. \end{aligned} \tag{A.5}$$

The complex envelope $\{s(t)\}$ can be written in terms of its real and imaginary parts as

$$s(t) = s_I(t) + j s_Q(t) \,. \tag{A.6}$$

From (A.5) and (A.6), we get

$$\begin{aligned} \tilde{s}(t) &= \sqrt{2}[s_I(t)\cos 2\pi f_c t - s_Q(t)\sin 2\pi f_c t] \\ &= \sqrt{2}\,a(t)\cos[2\pi f_c t + \psi(t)] \,, \end{aligned} \tag{A.7}$$

where

$$a(t) = \sqrt{s_I^2(t) + s_Q^2(t)}, \quad \text{and} \;\; \psi(t) = \tan^{-1}\frac{s_Q(t)}{s_I(t)} \,. \tag{A.8}$$

The signal $a(t)$ is called the (real) *envelope* of $s(t)$, and $\psi(t)$ is called the *phase* of $s(t)$. It is to be noted that every bandpass signal can be written in the forms given in (A.7).

A.2 COMPLEX BASEBAND REPRESENTATION OF CHANNEL RESPONSE

Referring to Figure 1.1, since the output of the channel $\tilde{y}(t)$ is a bandpass signal, it has the complex baseband representation

$$y(t) = \tilde{y}_+(t)\, e^{-j2\pi f_c t} \,. \tag{A.9}$$

The signal $\tilde{y}(t)$ is related to $\tilde{s}(t)$ through the convolution integral, i.e.,

$$\tilde{y}(t) = \tilde{h} \star \tilde{s}(t) = \int \tilde{h}(\tau)\; \tilde{s}(t-\tau) d\tau \,. \tag{A.10}$$

Equivalently

$$\tilde{Y}(f) = \tilde{H}(f)\; \tilde{S}(f) \tag{A.11}$$

It is of interest to see if the complex envelopes $s(t)$ and $y(t)$ are related in a similar fashion. It is easy to show that this is indeed the case. From (A.11),

$$\begin{aligned} Y(f) &= \tilde{Y}_+(f + f_c) \\ &= \sqrt{2}\;\tilde{Y}(f + f_c)\, u(f + f_c) \\ &= \sqrt{2}\;\tilde{H}(f + f_c)\;\tilde{S}(f + f_c)\, u(f + f_c) \\ &= \tilde{H}(f + f_c)\, u(f + f_c)\; S(f) \,. \end{aligned} \tag{A.12}$$

Thus we can write $Y(f)$ in terms of $S(f)$ as

$$Y(f) = H(f)\, S(f)\,, \tag{A.13}$$

with $H(f)$ defined as

$$H(f) = \frac{1}{\sqrt{2}} \tilde{H}_+(f + f_c)\,. \tag{A.14}$$

This implies that

$$h(t) = \frac{1}{\sqrt{2}} \tilde{h}_+(t)\, e^{-j2\pi f_c t} \tag{A.15}$$

and that

$$\tilde{h}(t) = 2\,\mathsf{Re}[h(t)\, e^{j2\pi f_c t}]\,. \tag{A.16}$$

Comparing (A.5) and (A.16), we see that there is an additional factor of $\sqrt{2}$ in the equation relating $h(t)$ and $\tilde{h}(t)$.

A.3 COMPLEX BASEBAND REPRESENTATION OF NOISE

We now consider the additive noise term $\tilde{w}(t)$ in Figure 1.1. Since every sample path of $\tilde{w}(t)$ is a bandpass signal, the random process $\tilde{w}(t)$ can be represented (almost surely) by a complex envelope which we denote by $w(t)$. Hence, $w(t)$ is a complex-valued random process and it is related to the process $\tilde{w}(t)$ as:

$$\begin{aligned} w(t) &= \tilde{w}_+(t)\, e^{-j2\pi f_c t} \\ &= \frac{1}{\sqrt{2}} \left[\tilde{w}(t) + j\hat{\tilde{w}}(t)\right] e^{-j2\pi f_c t} \end{aligned} \tag{A.17}$$

and

$$\tilde{w}(t) = \mathsf{Re}[\sqrt{2}\, w(t)\, e^{j2\pi f_c t}]\,. \tag{A.18}$$

The complex process $w(t)$ inherits several interesting properties from $\tilde{w}(t)$. We discussed these properties in Section 1.2.1.

A.4 BASEBAND MODEL

Based on the complex baseband representations of the signal, channel response and noise, we have the following complex baseband system shown in Figure A.2 which is equivalent to the bandpass system of Figure A.1. Note that $r(t)$ is the complex envelope of $\tilde{r}(t)$, i.e., $r(t) = \tilde{r}_+(t)\, e^{-j2\pi f_c t}$.

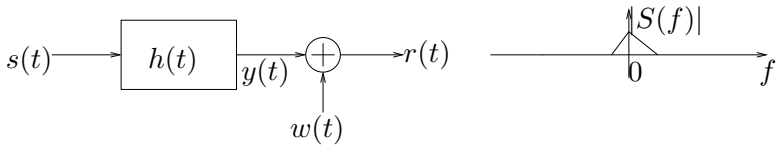

Figure A.2: Complex baseband model for point-to-point communications.

Appendix B

Proper Complex Random Processes

Remarkably, all the complex random processes we will be interested in studying in this book have the same elegant structure as the that of the baseband process $w(t)$ of Section 1.2.1. This structure that makes analysis in the complex baseband domain considerably more convenient than in the real passband domain. In this appendix we study this structure in more detail, following the development in the paper by Neeser and Massey [NM93].

B.0.1 PROPER COMPLEX RANDOM VECTORS

We begin by studying the symmetry structure in the simpler context of random finite-dimensional vectors. Let $\boldsymbol{Y} = \boldsymbol{Y}_I + j\boldsymbol{Y}_Q$ be a complex random n-vector. Since the components $\boldsymbol{Y}_I$ and $\boldsymbol{Y}_Q$ are real-valued, we may define the real auto- and cross-covariance matrices in the standard way as:

$$\begin{aligned}
\boldsymbol{\Sigma}_{\boldsymbol{Y}_I} &= \mathsf{cov}[\boldsymbol{Y}_I, \boldsymbol{Y}_I] = \mathsf{E}[(\boldsymbol{Y}_I - \boldsymbol{m}_{\boldsymbol{Y}_I})(\boldsymbol{Y}_I - \boldsymbol{m}_{\boldsymbol{Y}_I})^\top] \\
\boldsymbol{\Sigma}_{\boldsymbol{Y}_Q} &= \mathsf{cov}[\boldsymbol{Y}_Q, \boldsymbol{Y}_Q] = \mathsf{E}[(\boldsymbol{Y}_Q - \boldsymbol{m}_{\boldsymbol{Y}_Q})(\boldsymbol{Y}_Q - \boldsymbol{m}_{\boldsymbol{Y}_Q})^\top] \\
\boldsymbol{\Sigma}_{\boldsymbol{Y}_I\boldsymbol{Y}_Q} &= \mathsf{cov}[\boldsymbol{Y}_I, \boldsymbol{Y}_Q] = \mathsf{E}[(\boldsymbol{Y}_I - \boldsymbol{m}_{\boldsymbol{Y}_I})(\boldsymbol{Y}_Q - \boldsymbol{m}_{\boldsymbol{Y}_Q})^\top] \\
\boldsymbol{\Sigma}_{\boldsymbol{Y}_Q\boldsymbol{Y}_I} &= \mathsf{cov}[\boldsymbol{Y}_Q, \boldsymbol{Y}_I] = \mathsf{E}[(\boldsymbol{Y}_Q - \boldsymbol{m}_{\boldsymbol{Y}_Q})(\boldsymbol{Y}_I - \boldsymbol{m}_{\boldsymbol{Y}_I})^\top]
\end{aligned} \tag{B.1}$$

There are two ways to the define the covariance matrix of the complex vector Y. The (standard) covariance matrix is defined by:

$$\boldsymbol{\Sigma}_{\boldsymbol{Y}} = \mathsf{E}\left[(\boldsymbol{Y} - \boldsymbol{m}_Y)(\boldsymbol{Y} - \boldsymbol{m}_Y)^\dagger\right] . \tag{B.2}$$

But we may also define a quantity called the *pseudocovariance* matrix which is given by

$$\tilde{\boldsymbol{\Sigma}}_{\boldsymbol{Y}} = \mathsf{E}\left[(\boldsymbol{Y} - \boldsymbol{m}_Y)(\boldsymbol{Y} - \boldsymbol{m}_Y)^\top\right] \tag{B.3}$$

The difference between these two covariance matrices is that for the latter matrix the second term inside the expectation is not conjugated.

It is easy to express the complex covariance matrices in terms of the real covariance matrices of (B.1).

$$\begin{aligned}
\boldsymbol{\Sigma}_{\boldsymbol{Y}} &= \left(\boldsymbol{\Sigma}_{\boldsymbol{Y}_I} + \boldsymbol{\Sigma}_{\boldsymbol{Y}_Q}\right) + j\left(\boldsymbol{\Sigma}_{\boldsymbol{Y}_Q\boldsymbol{Y}_I} - \boldsymbol{\Sigma}_{\boldsymbol{Y}_I\boldsymbol{Y}_Q}\right) \\
\tilde{\Sigma}_{\boldsymbol{Y}} &= \left(\boldsymbol{\Sigma}_{\boldsymbol{Y}_I} - \boldsymbol{\Sigma}_{\boldsymbol{Y}_Q}\right) + j\left(\boldsymbol{\Sigma}_{\boldsymbol{Y}_Q\boldsymbol{Y}_I} + \boldsymbol{\Sigma}_{\boldsymbol{Y}_I\boldsymbol{Y}_Q}\right)
\end{aligned} \tag{B.4}$$

The motivation for defining the pseudocovariance matrix lies in the following definition:

Definition B.1. *$\boldsymbol{Y}$ is said to be a* proper *complex random vector if pseudocovariance matrix $\tilde{\Sigma}_Y = 0$.*

It follows from (B.4) that proper complex (PC) Y satisfies the following symmetry properties, which are similar to the properties we saw earlier in (1.3) for complex baseband additive noise:

$$\begin{aligned} \boldsymbol{\Sigma}_{\boldsymbol{Y}_I} &= \boldsymbol{\Sigma}_{\boldsymbol{Y}_Q} \\ \boldsymbol{\Sigma}_{\boldsymbol{Y}_Q \boldsymbol{Y}_I} &= -\boldsymbol{\Sigma}_{\boldsymbol{Y}_I \boldsymbol{Y}_Q} \, . \end{aligned} \tag{B.5}$$

It also follows from (B.4) that

$$\boldsymbol{\Sigma}_{\boldsymbol{Y}} = 2\boldsymbol{\Sigma}_{\boldsymbol{Y}_I} + j2\boldsymbol{\Sigma}_{\boldsymbol{Y}_Q \boldsymbol{Y}_I} \, . \tag{B.6}$$

The Scalar Case

In the special case where $\boldsymbol{Y}$ is a scalar, denoted by Y, it is clear that

$$\boldsymbol{\Sigma}_{Y_Q Y_I} = \mathsf{E}[(Y_I - m_I)(Y_Q - m_Q)] = \boldsymbol{\Sigma}_{Y_I Y_Q} \tag{B.7}$$

In this case, if Y is proper, which means that $\mathsf{E}[(Y - m_Y)^2] = 0$, then $\boldsymbol{\Sigma}_{Y_Q Y_I} = -\boldsymbol{\Sigma}_{Y_I Y_Q}$. This together with (B.7) implies that $\boldsymbol{\Sigma}_{Y_Q Y_I} = 0$, i.e. that Y_I and Y_Q are uncorrelated. Furthermore, from (B.6), we get

$$\boldsymbol{\Sigma}_Y = \sigma_Y^2 = \mathsf{E}[|Y - m_Y|^2] = 2\boldsymbol{\Sigma}_{Y_I} = 2\sigma_{Y_I}^2 = 2\sigma_{Y_Q}^2 \, . \tag{B.8}$$

Thus for a complex random scalar Y to be proper, the in-phase and quadrature components must have the same variance and be uncorrelated. Also we see that variance of Y is twice the variance of each of the components.

Important Results on Proper Complex Random Vectors

In the following, we give some general results for proper complex random vectors that also justify the use of the term "proper" in decribing such complex random vectors. The proofs are straightforward and are give in [NM93].

Result B.1. *[NM93] Let $\boldsymbol{Y}$ be a proper complex random n-vector, and suppose the random m-vector $\boldsymbol{Z}$ is defined by*

$$\boldsymbol{Z} = \boldsymbol{A}\boldsymbol{Y} + \boldsymbol{b} \, .$$

Then $\boldsymbol{Z}$ is also proper complex.

This result says that 'properness" is preserved under affine transformations.

Result B.2. *[NM93] Let $\boldsymbol{Y} = \boldsymbol{Y}_I + j\boldsymbol{Y}_Q$ be proper complex and Gaussian, i.e. $\boldsymbol{Y}_I, \boldsymbol{Y}_Q$ are jointly Gaussian. Then*

$$\begin{aligned} p_{\boldsymbol{Y}}(\boldsymbol{y}) &:= p_{\boldsymbol{Y}_I \boldsymbol{Y}_Q}(\boldsymbol{y}_I, \boldsymbol{y}_Q) \\ &= \frac{1}{\pi^n |\boldsymbol{\Sigma}_{\boldsymbol{Y}}|} \exp\left\{ -(\boldsymbol{y} - \boldsymbol{m}_Y)^\dagger \boldsymbol{\Sigma}_Y^{-1} (\boldsymbol{y} - \boldsymbol{m}_Y) \right\} \end{aligned} \tag{B.9}$$

In the equation above, $|\mathbf{\Sigma}_{\boldsymbol{Y}}|$ denotes the determinant of the matrix $\mathbf{\Sigma}_{\boldsymbol{Y}}$. Note that (B.9) does not hold if $\boldsymbol{Y}$ is not proper. For a general complex Gaussian vector $\boldsymbol{Y}$, the joint distribution of $\boldsymbol{Y}_I$ and $\boldsymbol{Y}_Q$ has to be written explicitely in terms of the auto- and cross-covariance matrices given in (B.1).

Proper complex Gaussian vectors are also called *circularly* complex Gaussian vectors. This is because the pdf of $\boldsymbol{Y}$ is unchanged if we rotate each component by some angle θ, i.e. $\boldsymbol{X} = e^{j\theta}\boldsymbol{Y}$ has the same pdf as Y. A proper complex Gaussian (PCG) distribution with mean $\boldsymbol{\mu}$ and covariance matrix $\mathbf{\Sigma}$ is denotes compactly as $\mathcal{CN}(\boldsymbol{\mu}, \mathbf{\Sigma})$.

Since Gaussianity and properness are preserved by affine transformations, we have the following corollary to Result B.1.

Corollary B.1. *If $\boldsymbol{Y}$ is a proper complex Gaussian (PCG) vector, then $\boldsymbol{Z} = \boldsymbol{A}\boldsymbol{Y} + \boldsymbol{b}$ is also a PCG vector.*

We now give a version of the Central Limit Theorem for proper complex random vectors.

Result B.3. *(Central Limit Theorem). Let $\{\boldsymbol{Y}_k\}_{k=1}^n$ be a sequence of independent and identically distributed proper complex random vectors (not necessarily Gaussian) with mean $\boldsymbol{\mu}$ and covariance matrix $\mathbf{\Sigma}$. Then the sum*

$$\frac{1}{\sqrt{n}} \sum_{k=1}^{n} (\boldsymbol{Y}_k - \boldsymbol{\mu})$$

converges in distribution to a $\mathcal{CN}(\mathbf{0}, \mathbf{\Sigma})$ random vector.

B.0.2 PROPER COMPLEX PROCESSES

Let $Y(t) = Y_I(t) + jY_Q(t)$ be a complex random process. Parallel to the vector case, we define covariance and pseudocovariance functions:

$$\begin{aligned} C_Y(t+\xi, t) &= \mathsf{E}\left[(Y(t+\xi) - m_Y(t+\xi))(Y(t) - m_Y(t))^\star\right] \\ \tilde{C}_Y(t+\xi, t) &= \mathsf{E}\left[(Y(t+\xi) - m_Y(t+\xi))(Y(t) - m_Y(t))\right] \end{aligned} \tag{B.10}$$

It is easy to show that

$$\begin{aligned} C_Y(t+\xi, t) &= [C_{Y_I}(t+\xi, t) + C_{Y_Q}(t+\xi, t)] + j[C_{Y_Q Y_I}(t+\xi, t) - C_{Y_I Y_Q}(t+\xi, t)] \\ \tilde{C}_Y(t+\xi, t) &= [C_{Y_I}(t+\xi, t) - C_{Y_Q}(t+\xi, t)] + j[C_{Y_Q Y_I}(t+\xi, t) + C_{Y_I Y_Q}(t+\xi, t)] \end{aligned} \tag{B.11}$$

Definition B.2. *$Y(t)$ is proper complex if the pseudocovariance $\tilde{C}_{YY}(t+\xi, t) = 0$, i.e., if*

$$C_{Y_I}(t+\xi, t) = C_{Y_Q}(t+\xi, t) \quad \textit{and} \quad C_{Y_Q Y_I}(t+\xi, t) = -C_{Y_I Y_Q}(t+\xi, t)$$

This is of course the symmetry property we saw earlier in (1.3) for complex baseband additive noise.

Note that for zero mean $Y(t)$, the covariance functions C above may be replaced by correlation functions R. Also, if $Y_I(t)$ and $Y_Q(t)$ are jointly WSS, then $Y(t)$ is WSS, and $(t+\xi, t)$ in the above equations may be replaced by ξ.

As in the vector case, for proper complex $Y(t)$,

$$C_Y(t+\xi, t) = 2C_{Y_I}(t+\xi, t) + j2C_{Y_Q Y_I}(t+\xi, t)\,. \tag{B.12}$$

The following result is easily established from Definition B.2

Result B.4. *[NM93] For any n, and any $t_1, \ldots, t_n$, the samples $Y(t_1), \ldots, Y(t_n)$ of a proper complex process $Y(t)$ form a proper complex random vector*

Now we define the most important class of proper complex processes for this book.

Definition B.3. *A proper complex process $Y(t)$ is said to be proper compex Gaussian (PCG) if, for all n, and all $t_1, t_2, \ldots, t_n$, the samples $Y(t_1), Y(t_2), \ldots, Y(t_n)$ form a proper complex Gaussian vector.*

The following result is the continuous-time version of Theorem B.1.

Result B.5. *[NM93] If a proper complex process $Y(t)$ is passed through a linear (possibly time-varying) system to form*

$$Z(t) = \int_{s=-\infty}^{\infty} h(t,s)Y(s)ds \; .$$

Then $Z(t)$ is proper complex as well. In addition, if $Y(t)$ is proper complex Gaussian, then $Z(t)$ is proper complex Gaussian as well.

Bibliography

[Cla68] Clarke R. (July-August 1968) A statistical theory of mobile radio reception. *Bell Syst. Tech. J.* 47(6): 957–1000.

[Gud91] Gudmundson M. (1991) Correlation model for shadow fading in mobile radio systems. *Electron. Lett.* 27(23): 2145–2146.

[HJ85] Horn R. A. and Johnson C. R. (1985) *Matrix Analysis*. Cambridge, New York.

[AS64] Abramowitz M. and Stegun I. A. (1964) *Handbook of Mathematical Functions*. Dover, New York.

[NM93] Neeser F. D. and Massey J. L. (July 1993) Proper complex random processes with applications to information theory. *IEEE Trans. Inform. Th.* 39(4).

[Par98] Parsons J. D. (1998) *The Mobile Radio Propagation Channel*. Wiley, Chichester, England.

[Bel63] P. A. Bello. Characterization of randomly time-variant linear channels. *IEEE Trans. Commun. Systems*, pages 360–393, December 1963.

[Pro95] Proakis J. G. (1995) *Digital Communications*. Mc-Graw Hill, New York, 3rd edition.

[Rap96] Rappaport T. S. (1996) *Wireless Communications: Principles and Practice*. Prentice Hall, Upper Saddle River, NJ.

[Ric48] Rice S. (January 1948) Statistical properties of a sine wave plus noise. *Bell Syst. Tech. J.* 27(1): 109–157.

[Stu96] Stuber G. (1996) *Principles of Mobile Communication*. Kluwer Academic, Norwell, MA.

[Jak74] Jakes, W. C., Jr. (1974) *Microwave Mobile Communications*. Wiley, New York.

[WH85] Wong E. and Hajek B. (1985) *Stochastic Processes in Engineering Systems*. Springer-Verlag, New York.

